ELSEVIER

Journal of Biomechanics 32 (1999) 1191–1197

JOURNAL OF BIOMECHANICS

www.elsevier.com/locate/jbiomech

Measuring muscle and joint geometry parameters of a shoulder for modeling purposes

Mary D. Klein Breteler[a,*], Cornelis W. Spoor[b,c], Frans C.T. Van der Helm[c]

[a]*Nijmegen Institute for Cognition and Information, P.O. Box 9104, 6500 HE Nijmegen, The Netherlands*
[b]*Department of Orthopaedics, University Hospital, Leiden, The Netherlands*
[c]*Department of Mechanical Engineering and Marine Technology, Delft University of Technology, The Netherlands*

Received 8 June 1998; accepted 6 June 1999

Abstract

An extensive set of muscle and joint geometry parameters was measured of the right shoulder of an embalmed male. For all muscles the optimal muscle fiber length was determined by laser diffraction measurements of sarcomere length. In addition, tendon length and physiological cross-sectional area were determined. The parameter set was needed to enhance the reliability of a computer model of the shoulder (Van der Helm, 1994a,b Journal of Biomechanics 27, 527–550, 551–569). With the model, an abduction of the arm was simulated in seven positions, at 30° intervals. In each of the simulated arm positions, actual sarcomere lengths were calculated from the lengths of 104 muscle elements, distributed over 16 shoulder muscles. For most muscle elements, the simulated abduction appeared to take place within the sarcomere length range in which the muscle elements can exert force. The muscle elements can then act on the ascending limb as well as on the plateau and on the descending limb of the relative force–length curves of sarcomeres. The produced data set is not only important for the refinement of shoulder modeling, but also for functional analyses of shoulder movements in general.

Keywords: Shoulder; Sarcomere length; Model

1. Introduction

The human shoulder is a very complex mechanism. Unlike quadrupeds the forelimbs of man are not primarily used for support of the body weight and locomotion but for manipulation. A stable base and a wide movement range for the upper arm are needed. Stability is provided for by a closed kinematic chain consisting of thorax, clavicula, and scapula (Fig. 1) in combination with muscles and ligaments. The motion range of the upper arm is favored by the shallow cavity of the glenoid and by the adaptation of the glenoid orientation to the humerus direction.

For studying the complex three-dimensional movements of the shoulder, several data sets have been measured (Högfors et al., 1987; Wood et al., 1989a,b; Van der Helm, 1994a,b; Johnson et al., 1996), and some computer models have been developed, based on the finite-element (FE) theory (Pronk, 1991; Van der Helm, 1991,1994a,b) or otherwise (Karlsson and Peterson, 1992). The shoulder model in the present paper is an extension of the shoulder model of Van der Helm (1994b). The latter also compared various models and gave a validation of the shoulder model.

Since our FE model has more muscle elements than the shoulder mechanism has degrees of freedom, muscle forces have to be calculated by means of an optimization procedure. Van der Helm (1994a,b) minimizes the sum of squared muscle stresses in the entire system. The magnitude of activation of a muscle element in his model depends on the moment arm and on the maximum possible force of the muscle element. The maximum force at a given muscle element length depends, apart from being proportional to the physiological cross-sectional area, on the optimum length of the muscle element, which, to date, was only approximated.

The purpose of this study was to measure additional muscle parameters that are needed for calculating the

* Corresponding author.
E-mail address: kleinbreteler@nici.kun.nl (M.D. Klein Breteler)

0021-9290/99/$ - see front matter
PII: S0021-9290(99)00122-0

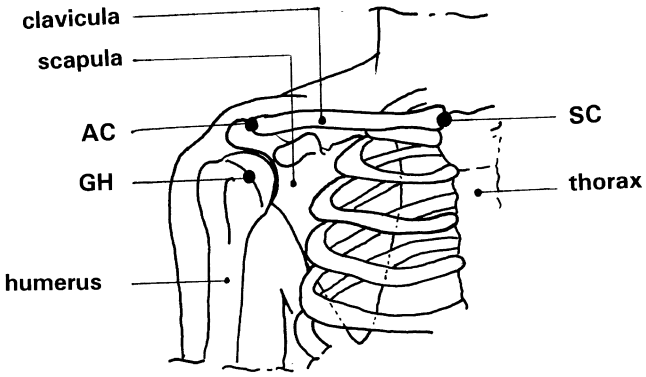

Fig. 1. The shoulder mechanism consists of the following skeletal entities: the thorax, clavicula, scapula, and humerus; and the following joints: the sternoclavicular joint (SC), acromioclavicular joint (AC) and glenohumeral joint (GH). Between thorax and scapula a scapulothoracic gliding plane is present.

optimum lengths of all modeled muscle elements, so that more reliable muscle force estimates are possible in the shoulder model (Van der Helm, 1994a,b). Tendon length and optimum fiber length are important parameters for accurate muscle modeling. Slack length of the tendon is calculated as the total muscle element length minus its fiber length. The parameters needed to calculate optimum fiber length are sarcomere length and muscle fiber length. Though these parameters are known for some body parts (for the lower limb see e.g. Wickiewicz et al., 1983), currently these parameters have never been measured before for a complete shoulder, which is a large-scale 3D musculoskeletal system. All parameters in our study have been measured on one specimen, so we may expect a consistent set (unlike in the case of averaging over several specimens). From the parameter set, input and model parameters for the shoulder model were calculated.

Subsequently, an abduction motion of the arm was simulated. From the relative muscle element lengths in each stage of the abduction, the forces that muscle elements can maximally exert at those lengths were calculated, according to the sarcomere force–length relationship (Walker and Schrodt, 1974).

This paper has two main parts. First, a description of the measurements of the parameter set will be given. Only part of the parameter set is presented here. The complete data set is available on the Internet (http://www-mr.wbmt.tudelft.nl/shoulder/morph_data). In the second part of this paper how the parameters were implemented in the shoulder model and how an abduction of the arm in seven steps of 30° was simulated are described. The simulation was performed to find out whether the muscles stayed within the length range in which they can exert force according to the force–length relationship.

2. Cadaver measurements: method and results

Measurements were performed on the right shoulder of an embalmed 57-year-old muscular man. Length and weight of the cadaver could not be determined since the lower body half had been removed before the cadaver became available. Total body length was estimated to be 168 cm with the help of proportional dimensions (Martin and Saller, 1957). The thorax and head were rigidly fixed inside a stainless steel frame, which allowed easy positioning of the specimen. In every part of the skeleton, i.e., head, thorax, clavicula, scapula, humerus, radius and ulna, four or five screws were driven. These screws were evenly and non-collinearly distributed over the bone, so that they could be used as reference points for measuring changes in position and orientation. Prior to dissection, the positions of four reference points on the frame, 18 palpable bony landmarks and all screws were measured. For measuring positions, we used the palpator (Pronk and Van der Helm, 1991; Veeger et al., 1991; Van der Helm et al., 1992), a 3D instrumented linkage digitizer with a standard deviation of 0.1 mm per co-ordinate.

Data are expressed in a global orthogonal co-ordinate system, with the incisura jugularis (IJ) as origin. The axes were defined as follows (see Table 1 for symbols):

y-axis: through the middle between IJ and C7 and the middle between PX and T8, pointing cranially.
auxiliary z-axis: C7–IJ.
x-axis: $\perp$ y-axis and auxiliary z-axis, pointing to the right.
z-axis: $\perp$ x-axis and y-axis, pointing backwards.

2.1. Palpable bony landmarks

Positions of palpable bony landmarks are not only needed for defining a global co-ordinate system, but also serve as input parameters for the shoulder model. In Table 1 the positions of the main palpable bony landmarks on thorax and scapula are given.

2.2. Muscle and ligament attachment sites

First the skin and the fatty tissues over and between the muscles were removed. Each muscle was cleared from its surrounding without disconnecting the origin or insertion. For each muscle it was decided as to how many elements it should be divided into. Criteria were: attachment sites on different bones, apparent differences in muscle fiber lengths, differences in the angle between muscle fiber and bone, attachment to another tendon plate, or gliding planes present between parts of the muscle. For each muscle element, the visually estimated centroid of the origin and insertion were marked with numbered labels, both on the bone and the muscle. For

Table 1
Positions of palpable bony landmarks (in cm) on the thorax and scapula

Palpable bony landmark	*X*	*Y*	*Z*
Incisura jugularis (IJ)	0	0	0
Processus xiphoideus (PX)	− 0.98	− 13.27	− 3.19
7th Cervical vertebra (C7)	0	5.41	12.42
1st Thoracal vertebra (T1)	0.14	3.62	13.68
8th Thoracal vertebra (T8)	0.98	− 17.15	15.61
Acromioclavicular fissura (AC)	16.50	2.66	7.14
Trigonum spinae (TS)	7.51	− 1.18	15.59
Angulus inferior (AI)	10.19	− 12.62	15.65

some muscles it was impossible to divide the muscle in situ, because part of the muscle was hidden or because no separate elements could be distinguished from outside. In those cases the complete muscle was cut loose and points on the attachment site were marked, both on the bone and on the muscle. Then the muscle was divided into elements, without separating the origins and insertions. Centroids of muscle element attachment were marked on the muscle. They were copied to the bone after the muscle was fitted back into its original position with the help of the numbered labels. See Table 2 for the measured muscles.

Positions of origin and insertion of the ligg. conoideum, trapezoideum, costoclaviculare, sternoclaviculare, and glenohumerale, were measured with the palpator after all ligaments were cut and the bones were separated. Finally, on every bone the reference screws and the attachment sites of all muscle elements were measured. In total, the 16 muscles were divided into 104 muscle elements.

2.3. Rotation centers

After all muscles had been removed, but before the ligaments were cut, measurements with the palpator were performed to determine the positions of the joint rotation centers. For the acromioclavicular (AC) and sternoclavicular (SC) joints, the positions of the reference screws at about 10 extreme postures per joint were measured. The postures were limited by ligaments or bony contact. The point that had the minimum distance to the various screw axes relating the postures, was chosen as rotation center.

A raster of points of maximally 3 mm distance evenly distributed over the complete surface of the glenohumeral (GH) joint was measured after all bones were separated. A sphere was fitted to the points on the articular surface of the humeral head. Another sphere was fitted to the points on the glenoid, using the radius of the humeral head. The position of the center of this sphere served as rotation center of the GH joint. For the humeroulnar joint the midpoint between the medial and lateral epicondyles was used as rotation center (See Table 3). The rotation centers of the SC and AC joints appeared to be inside the clavicula. For comparison also the centroids of the articular surfaces are given.

Table 2
All muscles measured, the number of muscle elements per muscle and the order in which they were measured

Muscle	# elements	Order elements
m. trapezius, scap.	11	Cranial–caudal
m. trapezius, clav.	2	Cranial–caudal
m. levator scapulae	2	Medial–lateral
m. pectoralis minor	4	Cranial–caudal
m. rhomboideus	5	Cranial–caudal
m. serratus anterior	12	Caudal–cranial
m. deltoideus, scap.	11	Medial–lateral
m. deltoideus, clav.	4	Lateral–medial
m. coracobrachialis	3	No order
m. infraspinatus	6	Caudal–cranial
m. teres minor	3	No order
m. teres major	4	Caudal–cranial
m. supraspinatus	4	Caudal–cranial
m. subscapularis	11	Cranial–caudal
m. biceps, caput longum	2	No order
m. biceps, caput breve	2	No order
m. triceps	4	No order
m. latissimus dorsi	6	Cranial–caudal
m. pectoralis major, thor.	6	Caudal–cranial
m. pectoralis major, clav.	2	Medial–lateral

Table 3
Positions of the rotation centers, expressed in the global co-ordinate system (in cm)

Rotation center	*X*	*Y*	*Z*
Sternoclavicular joint	2.25	− 0.80	2.45
Centroid surface SC	1.90	− 0.82	1.43
Acromioclavicular joint	13.50	1.69	8.28
Centroid surface AC	14.95	2.03	8.54
Glenohumeral joint	16.37	− 1.79	8.11
Elbow joint	17.63	− 30.49	10.66

2.4. Muscle parameters

With a muscle element on a flat support, its length between origin and insertion label was copied to a string, and measured with a ruler. From every muscle element three representative fiber bundles were taken of approximately 2 mm width, and their lengths were measured. Tendon length, assumed to be fixed, was calculated by subtracting muscle fiber length from the total muscle element length. Pennation angles were considered negligible, except for the m. triceps brachii.

Sarcomere length was measured by diffraction of a He–Ne laser beam of about 1 mm diameter (Young et al., 1990). Fiber bundle samples were positioned in the laser beam at a fixed distance from a scale to allow direct reading of the sarcomere length. Samples were about 1 cm long and very thin and had been eased apart under an operation microscope. The resolution of the sarcomere length was at best 0.05 μm, probably depending on the quality of the embalming process. For each fiber bundle three samples of sarcomere length at three locations were recorded.

2.5. Calculation of model parameters

The optimum fiber length was calculated as the fiber bundle length divided by the mean sarcomere length in that fiber bundle, multiplied by the optimum sarcomere length of 2.7 μm (Walker and Schrodt, 1974). Optimum fiber length of a muscle element was the mean of its three optimum fiber bundle lengths.

The physiological cross-sectional area of a muscle element at optimum length is a measure for the maximum force that a muscle element can exert. It was calculated as the mass divided by the density, resulting in muscle volume, and subsequently divided by the optimum fiber length of that muscle element. Muscle elements were wiped with tissue to remove excess fluid before weighing. The specific density of muscle tissue (1.0576 g/cm^3) was determined by submerging a set of shoulder muscles.

One sphere through the humeral head, another sphere through the combined tubercula majus and minus, an ellipsoid through the thorax and a cylinder through the humerus shaft were fitted to the measured points on the respective surfaces. The parameters of these spheres, cylinder and ellipsoid, which represented bony contours causing muscle curvature, are given in Table 4. The ellipsoid also serves as scapulothoracic gliding plane, constraining the motions of the scapula.

Table 4
Bony contours. Mx, My and Mz are the co-ordinates of the centers of the sphere and ellipsoid (in cm). R is the radius. Ax, Ay and Az are the half axes of the ellipsoid. [dx dy dz] is the direction of the central axis of the cylinder. sx, sy and sz are the co-ordinates of an arbitrary point on the central axis of the cylinder

	Mx	My	Mz				R
Sphere 1	17.18	− 1.99	6.22				2.72
Sphere 2	17.08	− 1.79	6.50				2.44
	sx	sy	sz	dx	dy	dz	
Cylinder	15.56	0.03	− 1.51	− 0.01	19.82	− 8.54	0.90
	Mx	My	Mz	Ax	Ay	Az	
Ellipsoid	0.67	− 13.95	6.72	13.91	19.82	− 8.54	

Table 5
Segment moment of inertia (kg m^2) about a transversal axis I_t, and about a longitudinal axis I_l (Hinrichs, 1985), mass of the body segments (kg) and the positions of the mass centers (cm)

Body segment	I_t	I_l	mass	X	Y	Z
Thorax	—	—	—	0	− 13.93	6.80
Clavicula	0.001	0.003	0.156	8.44	1.22	6.80
Scapula	0.007	0.007	0.704	11.87	− 2.53	11.74
Upper arm	1.320	0.199	2.052	17.44	− 13.31	8.74
Forearm	0.612	0.091	1.093	18.69	− 43.84	12.21
Hand	0.064	0.019	0.525	21.45	− 61.09	11.78

Moments of inertia about a transversal and about a longitudinal axis were calculated with an equation of Hinrichs (1985). Segment mass centers were taken from Clauser et al. (1969). See Table 5.

3. Simulations: method and results

After implementation of the model parameters in the shoulder model (Van der Helm, 1994a), seven static postures as 30° intervals from an abduction motion were simulated. The input position data were obtained from bone orientations averaged over 10 living subjects (Van der Helm and Pronk, 1995). The same input data were used for comparison with earlier measurements and simulations (Van der Helm, 1994b). Input variables for the model were the y- and z-co-ordinates of AC, the y-co-ordinate of TS, the Euler angles of the humerus, and the external forces due to gravity. Euler angles of bone orientations were expressed relative to the virtual reference position, which was defined as a position in which the sternum, clavicula and scapula were aligned with the global co-ordinate system (Van der Helm, 1997).

Given the input variables and the motion constraint of the scapulothoracic gliding plane, the output parameters of the shoulder model (Van der Helm, 1994a) are: bone orientations, muscle lengths, muscle force vectors, moment arms, and muscle and joint moments. The output parameters are all in the dimensions of the cadaver. To get an impression of the contribution of the clavicula, scapula, and humerus to the abduction of the arm, see Van der Helm (1994a). The output parameter on which the remaining part of this paper is based is muscle length.

3.1. Maximal relative forces during abduction

Fiber length was calculated as the muscle element length minus the (constant) tendon length. The actual sarcomere length was obtained by dividing the fiber length by the optimum fiber length and then multiplying with the optimum sarcomere length, which is 2.7 μm. For

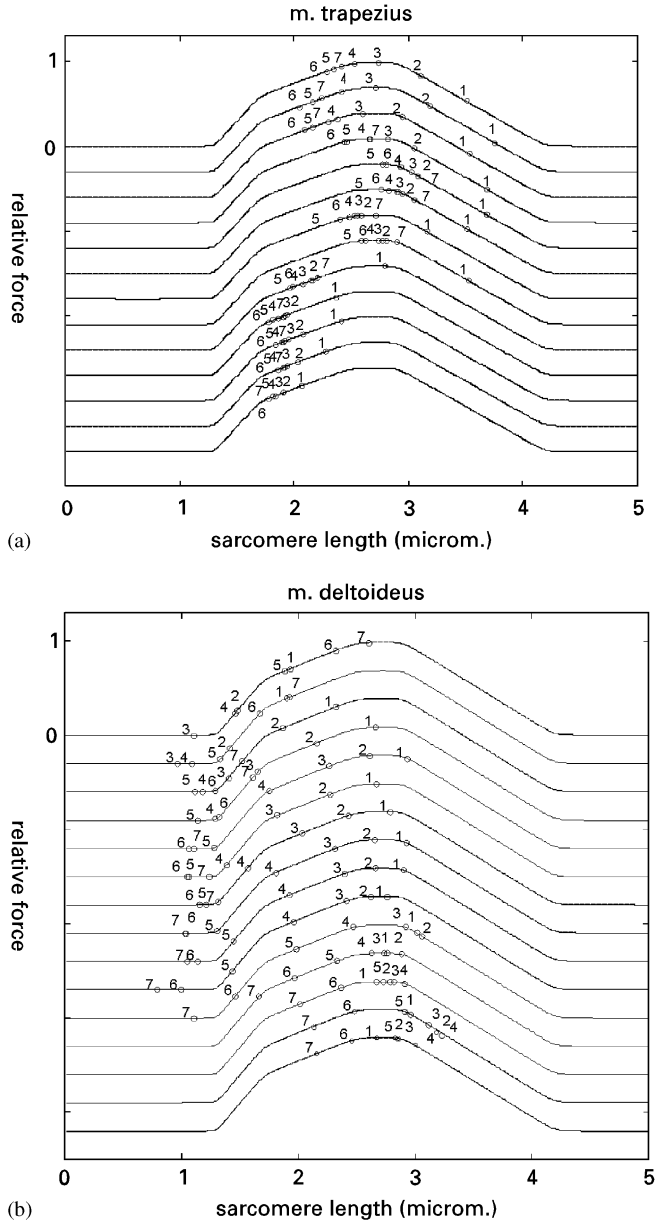

Fig. 2. (a) Relative maximum forces in 13 elements of the m. trapezius. The force–length curves are placed above each other for ease of comparison. The top curve is for the most cranial element, the bottom curve for the most caudal element. The x-axis gives the mean length of the sarcomeres (in μm) of a muscle element, and the y-axis, which is only valid for the top curve, gives the relative force that a muscle element can exert, ranging between 0 and 1. The numbers 1–7 denote the position during the abduction. Position 1 is with the arm down and position 7 is with the arm raised upright. (b) Relative maximum forces in 15 elements of the m. deltoideus. The top curve represents the most medial element of the posterior part of the muscle, the bottom curve the most medial element of the ventral part. The lower four elements represent the clavicular part. See (a) for more explanation.

the seven abduction postures, the actual sarcomere length and the relative maximum force of each muscle element were calculated. Figs. 2a and b show the force–length curves of all elements of the m. trapezius and m. deltoideus. The relative maximum forces (i.e., for maximum activation) in all seven stages of abduction are denoted. It can be seen that all muscle elements of the trapezius can exert force during the complete range of abduction; they shorten during abduction up to 150° (occasionally 120°) and lengthen in the final abduction stage. This means that in the first six positions of the abduction, all trapezius muscle elements can do positive work. The pattern is not exactly the same for all muscle elements, but it changes gradually over adjoining muscle elements. The middle part of the m. trapezius (pars transversus) has longer sarcomeres than the upper (pars descendens) and lower part (pars ascendens). This could be related with different functions for the three trapezius parts. In Fig. 2b, the striking feature is that at 120° and higher, most muscle elements of the scapular part of the m. deltoideus are too short to exert any force at all. This means that, above 120° abduction, another muscle is needed to lift the arm, for example the clavicular part of the m. deltoideus, or the clavicular and some cranial sternal elements of the m. pectoralis major which pass cranially from the glenohumeral abduction axis above 120°. According to Herring et al. (1984), the optimum length of a muscle is supposed to be adjusted to the position at which the muscle is activated most. Since optimum length was not attained at the same abduction position for all muscles, and even for the muscle elements within some muscles, it can be inferred that some muscles (or parts of a muscle) might be more active in the beginning of the abduction and other muscles are more active later on. This is probably also related to the actual moment arms during abduction.

4. Discussion

4.1. The measurements

The shoulder model calculates the shortest distance between origin and insertion, mostly straight but for some muscles around a bony contour. One would expect that the measured muscle length and the calculated distance between origin and insertion are nearly the same. However, differences of up to 5 cm were found for some elements of the m. latissimus dorsi. In Table 6 the measured muscle element lengths of the m. trapezius and m. deltoideus are given, and the muscle element lengths in the same posture according to the model. Within a muscle, the element length differences were highly correlated with spatial position, which points to a systematic causality. Several possible causes were considered.

Firstly, some muscle elements were markedly wrinkled in situ: the two cranial elements of the m. latissimus dorsi, the m. teres major and the two caudal elements of the m. pectoralis major.

Table 6
Measured muscle length versus modeled muscle length (in cm) for the m. trapezius and the m. deltoideus

Element number	m. trapezius		m.deltoideus	
	Measured	Modeled	Measured	Modeled
1	15.3	17.1	18.9	16.2
2	14.1	16.3	16.7	14.4
3	16.1	17.2	14.4	13.4
4	15.1	16.0	11.3	11.2
5	12.7	13.8	10.9	10.8
6	12.0	12.6	14.8	14.3
7	11.6	11.4	16.3	16.0
8	11.9	12.6	14.5	14.2
9	13.1	12.0	15.5	15.2
10	15.2	13.0	15.6	14.4
11	16.3	14.4	14.0	13.5
12	20.2	17.3	15.3	14.4
13	23.0	20.1	19.0	17.7
14			15.8	15.4
15			17.8	16.7

Secondly, bone positions had been measured with the specimen upright and the arm hanging down. The contralateral intact shoulder appeared to descend elastically about 2 cm in a similar situation. Therefore, elastic muscle length changes must be expected as compared to the unloaded muscle during length measurements. The effect is illustrated by the m. trapezius: the measured lengths of the cranial elements are about 2 cm less than the modeled lengths, in the middle the difference is small, and the caudal elements are about 3 cm longer (Table 6).

Thirdly, some muscle curvatures are not or not fully accounted for in the model. E.g., the length differences for the clavicular elements of the m. deltoideus can be quantitatively explained from their curvature.

For further calculations of tendon length, the measured muscle lengths were used.

Sarcomere lengths between 1.8 and 4.2 μm were measured, which is also the range that Walker and Schrodt (1974) argued to be consistent with the sliding filament theory. This makes it plausible that filament lengths have not changed during the embalming process. Sample preparation did not permanently alter sarcomere length. After overstretching some samples during length measurements in the laser beam, returned to their original lengths. In some muscle elements, a few samples with very small sarcomere lengths of 1.3 and 1.4 μm were found. These were considered artifacts and were further ignored, since (i) many samples with sarcomere lengths of 1.8 μm or longer were found in the same element, and (ii) no lengths were found between 1.4 and 1.8 μm. Assumably, it concerns muscle fibers broken during rigor mortis.

4.2. Modeling muscles and joints: differences between former and present shoulder models

In the former shoulder model (Van der Helm, 1991; Van der Helm and Veenbaas, 1991), muscles were represented by up to 6 elements of equal strength. In the present model, more elements are used (up to 15) for wide, flat muscles, and the force of each element is proportional to its PCSA. Comparison of the two representations for the m. serratus anterior showed a difference in the PCSA of maximally 1 cm^2 between the two representations. For the m. trapezius the difference in PCSA according to both methods was even less, so the method used in the earlier modeling was acceptable.

In the former model, the rotation centers for the SC and AC joints were assumed to be at the center of the articular surfaces. In the present model, the rotation centers followed the bone marker positions for various joint postures. After simulations with both rotation centers, it was found that there is not much difference between a movement with rotation centers on the articular surfaces and that calculated from screw axes. The difference at the angulus inferior for maximum abduction was only about 2 mm. So, positioning the rotation center in the optical centroid of the articular surface of SC or AC was a reasonable approximation.

In conclusion, an extensive parameter set of a human shoulder has been collected and has been incorporated in a shoulder model. A relevant improvement has been achieved in the potential for muscle force estimation and therefore muscle function analysis by means of the shoulder model. A simulation based on the parameter set showed that optimum length of the various muscles was attained at different abduction positions. Some (parts of) muscles might be more active in the beginning of the abduction and other muscle parts might be active later on.

Acknowledgements

The present study was performed under supervision of the Dutch Shoulder Group, a collaboration between the affiliations of the co-authors and the Institute for Fundamental and Clinical Human Movement Sciences, Free University Amsterdam. The authors wish to thank the Laboratory for Anatomy and Embryology (Head: Dr. A.C. Gittenberger-de Groot) of the Leiden University for offering the facilities to perform specimen preparations and Dr. Ruud Meulenbroek from the Nijmegen Institute of Cognition and Information for his comments on earlier drafts of this paper.

References

Clauser, C.E., McConville, J.T., Young, J.M., 1969. Weight, volume and center of mass of segments of the human body. Wright-Patterson Air Force Base Ohio (AMRL-TR-69-70). pp. 339–356.

Herring, S.W., Grimm, A.F., Grimm, B.R., 1984. Regulation in sarcomere number in skeletal muscle: a comparison of hypotheses. Muscle and Nerve 7, 161–173.

Hinrichs, R.N., 1985. Regression equations to predict segmental moments of inertia from anthropometric measurements: an extension of the data of Chandler et al. (1975). Journal of Biomechanics 18, 621–624.

Högfors, C., Sigholm, G., Herberts, P., 1987. Biomechanical model of the human shoulder — I. Elements. Journal of Biomechanics 20, 157–166.

Johnson, G.R., Spalding, D., Nowizke, A., Bogduk, N., 1996. Modeling the muscles of the scapula: morphometric and coordinate data and functional implications. Journal of Biomechanics 29, 1039–1051.

Karlsson, D., Peterson, B., 1992. Towards a model for force prediction in the human shoulder. Journal of Biomechanics 25, 189–199.

Martin, R., Saller, K., 1957. Lehrbuch der Anthropologie. Fischer, Stuttgart.

Pronk, G.M., 1991. The shoulder girdle. Doctoral Thesis, Delft University of Technology, ISBN 90-370-0053-3.

Pronk, G.M., Van der Helm, F.C., 1991. The palpator: an instrument for measuring the positions of bones in three dimensions. Journal of Medical Engineering and Technology 15, 15–20.

Van der Helm, F.C.T., 1991. The shoulder mechanism, a dynamic approach. Doctoral Thesis, Delft University of Technology, ISBN 90-370-0055-X.

Van der Helm, F.C.T., Veenbaas, R., 1991. Modeling the mechanical effect of muscles with large attachment sites: application to the shoulder mechanism. Journal of Biomechanics 24, 1151–1163.

Van der Helm, F.C.T., Veeger, H.E.J., Pronk, G.H., Van der Woude, L.H.V., Rozendal, R.H., 1992. Geometric parameters for musculoskeletal modeling of the shoulder system. Journal of Biomechanics 25, 129–144.

Van der Helm, F.C.T., 1994a. Analysis of the kinematic and dynamic behavior of the shoulder mechanism. Journal of Biomechanics 27, 527–550.

Van der Helm, F.C.T., 1994b. A finite element musculoskeletal model of the shoulder mechanism. Journal of Biomechanics 27, 551–569.

Van der Helm, F.C., Pronk, G.M., 1995. Three-dimensional recording and description of motions of the shoulder mechanism. Journal of Biomechanical Engineering 117, 27–40.

Van der Helm, F.C.T., 1997. A standardized protocol for motion recordings of the shoulder. In: Veeger, H.E.J., Van der Helm, F.C.T., Rozing, P.M. (Eds.), Proceedings of the First Conference of the International Shoulder Group, 26-27 August 1996. Delft University of Technology, Shaker Publishing BV, Maastricht, The Netherlands. ISBN 90-423-0008-6.

Veeger, H.E.J., Van der Helm, F.C.T., Van der Woude, L.H.V., Pronk, G.M., Rozendal, R.H., 1991. Inertia and muscle contraction parameters for musculoskeletal modeling of the shoulder mechanism. Journal of Biomechanics 24, 615–629.

Walker, S.M., Schrodt, G.R., 1974. I segment lengths and thin filament periods in skeletal muscle fibers of the rhesus monkey and the human. Anatomical Record 178, 63–82.

Wickiewicz, T.L., Roy, L.L., Powell, P.L., Edgerton, V.R., 1983. Muscle architecture of the human lower limb. Clinical Orthopaedics 179, 275–283.

Wood, J.E., Meek, S.G., Jacobsen, S.C., 1989a. Quantitation of human shoulder anatomy for prosthetic arm control — I. surface modeling. Journal of Biomechanics 22, 273–292.

Wood, J.E., Meek, S.G., Jacobsen, S.C., 1989b. Quantitation of human shoulder anatomy for prosthetic arm control — II. Anatomy matrices. Journal of Biomechanics 22, 309–325.

Young, L.L., Papa, C.M., Lyon, C.E., George, S.M., Miller, M.F., 1990. Comparison of microscopic and laser diffraction methods for measuring sarcomere lengths of contracted muscle fibers of chicken pectoralis major muscle. Poultry Science 69, 1800–1802.